




## Probing free-carrier and exciton dynamics in a bulk semiconductor with two-dimensional electronic spectroscopy

Jonas Allerbeck <sup>1,2</sup>, Thomas Deckert <sup>1</sup>, Laurens Spitzner,<sup>2</sup> and Daniele Brida <sup>1,2,\*</sup>

<sup>1</sup>*Université du Luxembourg, 162a, avenue de la Faïencerie, L-1511 Luxembourg, Luxembourg*

<sup>2</sup>*University of Konstanz, Universitätsstraße 10, 78457 Konstanz, Germany*



(Received 11 May 2021; revised 8 November 2021; accepted 9 November 2021; published 24 November 2021)

We employ partially collinear two-dimensional electronic spectroscopy to disentangle precisely the ultrafast dynamics of excitons and free carriers in gallium selenide. Femtosecond temporal and meV energy resolution in the visible spectral region allows us to observe ultrafast bleaching at the exciton resonance with a relaxation time of 112 fs that corresponds to the thermal dissociation of excitons at room temperature, and is orders of magnitude faster than carrier relaxation in the bulk crystal. Our method is applicable to other functional materials, two-dimensional systems, and nanostructures.

DOI: [10.1103/PhysRevB.104.L201202](https://doi.org/10.1103/PhysRevB.104.L201202)

The development of future semiconducting devices operating at high frequency and interfacing with fast optical modulation depends on the detailed understanding of nonequilibrium carrier dynamics in semiconductors at the fundamental level. These efforts target in particular two-dimensional materials [1,2] and functional hetero- or nanostructures [3], whose optical properties can be engineered to match a wide range of applications. Ultrafast spectroscopy is an established technique for the investigation of carrier dynamics following an impulsive photoexcitation in a condensed matter system [4]. However, the broadband nature of ultrafast pulses prevents intrinsically the precise energy resolution of the excitation process. To disentangle energetic correlations, quasiparticles, and the interplay of resonances within the spectral profile of ultrafast pulses, two-dimensional (2D) spectroscopy employing a sequence of three or more pulses must be applied [5]. It is a powerful technique that has been widely used to study the coupling of molecular resonances in the infrared [6,7], however, its application to femtosecond dynamics of solid state materials is still new [8,9]. Recent studies on functional materials show the exciton dissociation measured by 2D spectroscopy, for example in epitaxial quantum wells [10–12], nanocrystals [13], hybrid organic-inorganic perovskite materials [14,15], or organic semiconductors [16,17]. The investigation of ultrafast carrier dynamics in classic inorganic semiconductors with full access to the excitation dynamics is an important step towards developing modern photonic devices. Mapping the small relative changes in an electronic system whose optical properties are defined by continuum states and many-body interaction instead of individual molecular resonances [18] requires high sensitivity of the optical setup.

In this work, we present 2D electronic spectroscopy experiments with sub-10 fs time and 2 THz (8 meV) energy

resolution, probing the ultrafast carrier dynamics in bulk gallium selenide (GaSe), a layered semiconductor with a band gap of approximately 2 eV. With this example, we target a material with high technological relevance for nonlinear optics applications [19–21] as well as photonic sensing devices [22,23]. Motivated by the counterintuitive excitonic suppression [24] and interlayer coupling [25] when approaching the few-layer limit, we measure the ultrafast relaxation of room temperature excitons in an optically thin crystal of GaSe ( $\epsilon$ -polytype) with distinct access to the excitation energy paving the way to future investigation of few-layer samples and other 2D materials with impact for novel optoelectronic devices [26]. Previous 2D spectroscopy studies on GaSe have investigated excitonic coupling, providing precise information of temperature dependent linewidth and exciton ground state splitting [27], however these measurements lack spectral bandwidth and temporal resolution to resolve the dynamic evolution and the coupling to the continuum of the electronic wave functions within the band structure. Our partially collinear three-pulse experiment reveals the transient absorption change as a function of excitation and detection energy, allowing us to disentangle exciton (E) and free-carrier (FC) dynamics despite the broadband excitation pulse, and mapping the complex many-body interactions in this transient state. We extract the exciton lifetime  $\tau_E = 112(\pm 8)$  fs at resonant excitation  $E_E = 2$  eV, describing the ultrafast dissociation of excitons as depicted in Fig. 1(a).

Our experimental setup is based on a commercial Yb:KGW amplifier operating at 50 kHz repetition rate [4]. Broadband pump pulses are generated by a noncollinear optical parametric amplifier (NOPA) and transformed to a collinear phase-locked pulse pair with variable delay by an in-path interferometer based on birefringent wedges (TWINS) [28]. We use a white light supercontinuum as probe pulses, which are resolved in a high-speed spectrograph operating at the full repetition rate of the laser [4]. Custom chirped mirrors achieve pulse durations <10 fs for pump and probe pulses despite high material dispersion in the interferometer, which is

\*Corresponding author: [daniele.brida@uni.lu](mailto:daniele.brida@uni.lu)

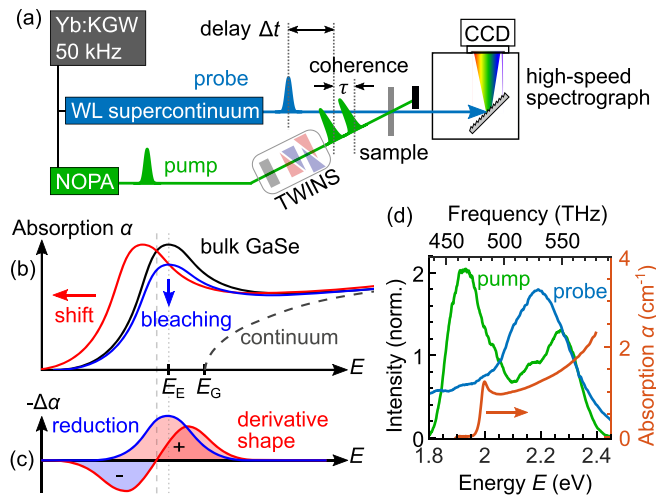


FIG. 1. (a) Sketch of the partially collinear 2D experiment and time ordering of pulses. TWINS: in-path interferometer; WL: white light; NOPA: noncollinear optical parametric amplifier. (b) Linear absorption  $\alpha$  and (c) differential transmission signal  $\Delta T/T \propto -\Delta\alpha$  illustrating dynamic changes observed in the experiment (see text). (d) Normalized pulse spectra and measured absorption of bulk GaSe at room temperature.

shorter compared to the investigated dynamics. The spectrometer resolution is 0.4 THz (2 meV) and excitation dynamics can be resolved with up to 1 THz (4 meV), limited by the scan range of the TWINS interferometer. Figure 1(a) schematically depicts the pulse sequence and relative delays of the experiment. Owing to the combination of high pulse energy and good counting statistics, our system provides an ideal platform to investigate many-body interactions connected to population dynamics in solid state functional materials. In this configuration, the probe pulse itself acts as a local oscillator for precise phasing of the emitted signal and subcycle phase stability between pump pulses enables long-term stability on the order of days without active stabilization.

GaSe features a strong excitonic resonance even at room temperature mediated by the strong binding energy of 10 meV [29,30]. Such strongly bound exciton transition is due to the relatively flat dispersion of valence and conduction band originating from the layered structure of the lattice [31]. In the linear absorption spectrum [black line in Fig. 1(b)] the exciton is revealed by the absorption peak at  $E_E$ , just below the fundamental band gap of free carrier excitation  $E_G$ . Differential absorption of the bulk sample can be linked to the dynamic change of transmission measured in the experiment:  $-\Delta\alpha \propto \Delta T/T$ . A gray dashed line in Fig. 1(b) schematically indicates the continuum absorption by free-carrier interband excitations. In a typical pump-probe experiment, upon impulsive photoexcitation, the signal associated to the excitonic absorption peak in GaSe bleaches and redshifts. This is the result of competing processes including Coulomb screening [32] and many-body effects induced by free carriers that renormalize the linear absorption profile on ultrafast time scales [33]. In addition, the depopulation of states near the band edge can reduce transiently the absorption at the exciton resonance. In a differential spectrum [Fig. 1(c)] the observed effects relate to a derivate-shape feature (shift, red line) and bleaching of the

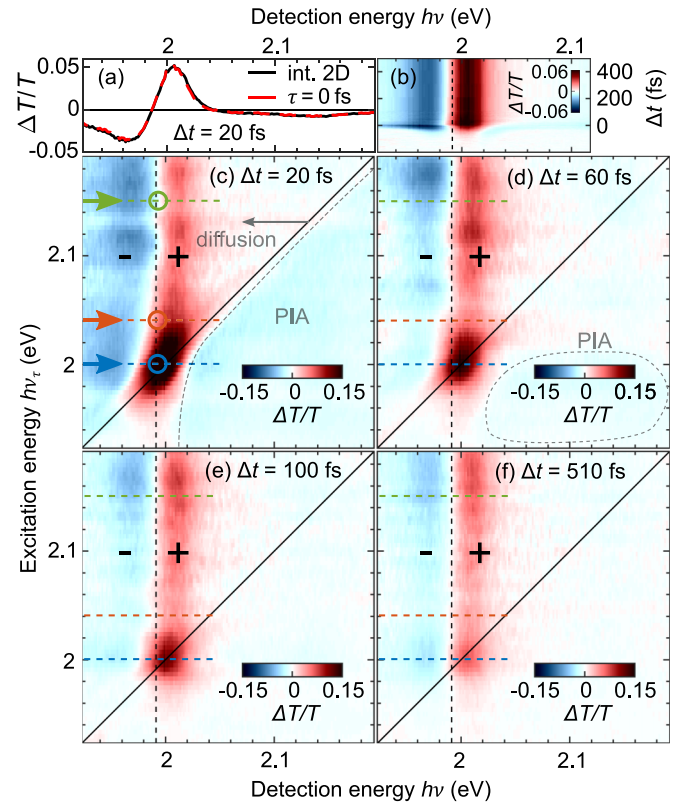


FIG. 2. 2D spectra of differential transmission change ( $\Delta T/T$ ) as a function excitation and detection energy. (a) Spectral profiles obtained by integrating the 2D map over the excitation energy (black) and for  $\tau = 0$  fs (red, dashed) as discussed in the text. (b) Standard pump-probe spectrum obtained at fixed  $\tau = 0$  fs. (c)–(f) 2D spectra at increasing delay time  $\Delta t$ . Red (+) and blue (–) areas show induced transparency (bleaching) and photoinduced absorption (PIA) respectively. Colored dashed lines and circles highlight excitation energies for the analysis of temporal dynamics. Solid black lines mark the spectral diagonal and dashed lines at  $h\nu = 1.99$  eV serve as a guide to the eye.

optical transitions (blue line). Importantly, these two distinct spectral signals overlap and clutter the spectroscopic investigation, rendering extremely difficult their precise untangling for the extraction of the timescales at which they occur. Hence, the detailed understanding requires a multidimensional spectroscopy approach that allows the decluttering of the signal at frequency neighboring the excitonic transition while preserving the temporal resolution.

For these reasons, we perform the 2D spectroscopy investigations on a free-standing 2- $\mu\text{m}$ -thick flake of  $\varepsilon$ -GaSe, which provides an ideal compromise of a large optical response and sufficient transmissivity at resonant photon energies. Figure 2 shows two-dimensional (2D) maps of differential transmission change  $\Delta T/T$  color coded as a function of detection ( $h\nu$ , horizontal axis) and excitation energy ( $h\nu_\tau$ , vertical axis) as well as increasing pump-probe delay time  $\Delta t$  in different panels (c)–(f). These spectra are obtained by scanning the pump pulse interference  $\tau$  at fixed delay  $\Delta t$  and recording the spectrally resolved relative transmission of probe pulses, hence expanding lines of fixed delay  $\Delta t$  from the standard pump probe spectrum [Fig. 2(b)] by an excitation axis with 2 THz

(8 meV) spectral resolution. Through appropriate phasing and calibration measurements the real part of the Fourier transform along the coherence time  $\tau$  yields the excitation energy [28]. Differential transmission of the 2D spectra is scaled in a two-step procedure. At first the 2D differential transmission is rescaled such that the spectral integration (average) along the excitation axis of 2D spectra (black) matches the differential profile measured at  $\tau = 0$  fs (red, dashed), before performing the Fourier transform [Fig. 2(a)]. The perfect agreement of both spectral profiles emphasizes that the 2D spectra fully contain and only expand the information obtained in standard pump-probe experiments (single excitation pulse) by adding the excitation axis. In a second step, the resulting spectrum is normalized along the vertical axis by the spectral intensity profile of the excitation pulse to account for different spectral weight. For this, we scale the average spectral intensity of the excitation pulse in the range 1.8–2.45 eV to unity. As a result, the maximum amplitude of differential transmission change in the 2D spectrum can exceed the maximum modulation  $\Delta T/T = 0.05$  of the integrated spectrum [Fig. 2(a)]. This emphasizes the role of competing effects at different excitation energy that can be extracted in the 2D spectrum, while they cancel out in a standard pump-probe experiment. In fact, the 2D spectrum at  $\Delta t = 20$  fs [Fig. 2(c)] disentangles the continuum response, showing photoinduced absorption (PIA) below and a positive signal above the diagonal. While PIA relates to the renormalization of continuum absorption [Fig. 1(b)], the temporal evolution of 2D maps shows clearly bleaching on the diagonal that diffuses towards lower detection energies as expected by thermalization of the free carriers and visible in the region above the diagonal that is characterized by weak positive signal. It should be noted that the signal associated to free carriers is rather faint due to the large density of states and the weak pump excitation. The integrated response of free carriers in a pump-probe measurement [Fig. 2(b)] is restricted to very short delays and remains at its peak one order of magnitude weaker, providing a measure for the instrument response with full width at half maximum (FWHM)  $< 30$  fs centered at  $\Delta t = 0$  fs.

Colored arrows and horizontal dashed lines in the 2D spectra in Fig. 2 highlight specific excitation energies: resonant exciton excitation at 2 eV (blue), free carrier interband excitations at high photon energy  $> 2.1$  eV (green), and the intermediate regime (red). The fluence of the excitation pulse employed in the experiment is  $1.5 \text{ mJ/cm}^2$  in free space, corresponding to an approximate photocarrier density of  $1.4 \times 10^{18} \text{ cm}^{-3}$  [34]. At this fluence two-photon excitation remains negligible as no differential signal is present at energies below 1.98 eV. The maximum relative change of transmission of the integrated spectrum is on the order of 0.05, matching to the differential pump-probe spectrum at  $\tau = 0$  fs [Fig. 1(a)]. All panels in Fig. 2 show a derivative-shape differential signal along the horizontal axis that represents the dynamic renormalization shift of the exciton resonance as sketched in Fig. 1(c). The vertical extension of this transient signal towards high excitation energy emphasizes the dominant optical response of the excitonic resonance due to renormalization effects, while the diagonal response [35] due to direct Pauli blocking remains negligible in comparison. At short delays  $\Delta t < 500$  fs [Fig. 2(c)–2(e)] this signal is superimposed by

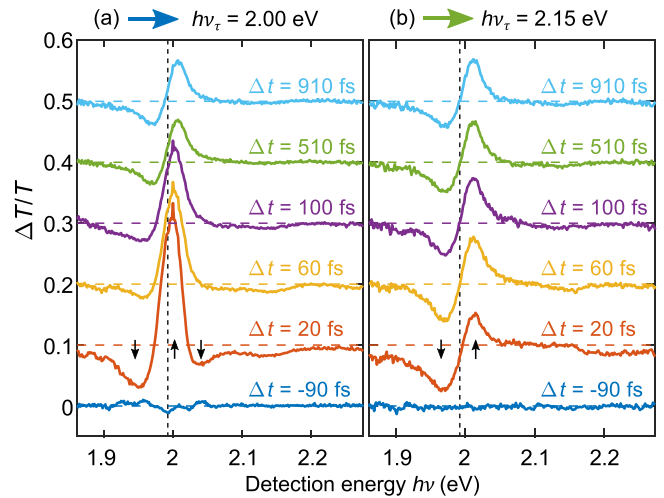


FIG. 3. Horizontal slices from the 2D maps in Fig. 2 highlight the temporal evolution of differential absorption spectra at specific excitation energy: (a) at the exciton resonance  $h\nu_\tau = 2 \text{ eV}$ , and (b) at photon energies higher than the band gap  $E_G$ . A vertical dashed line marks the detection energy  $h\nu = 1.99 \text{ eV}$  as a guide to the eye. Black arrows highlight transient dynamics as discussed in the main text.

a strong enhancement of the differential transmission (red). This ultrafast bleaching is distinct to photon energies near the excitonic resonance at 2 eV, and hence a measure for the total exciton population [3,36,37]. In condensed matter systems, optically excited excitons may also scatter out of the light cone, i.e., to dark excitons with nonzero center-of-mass [38]. However, the main signal observed in the experiments is due to the renormalization and bleaching of the direct exciton transition caused by all quasiparticles created by the excitation and as such is insensitive to the excitonic character.

The waterfall plots in Fig. 3 compare the temporal evolution of ultrafast bleaching at two distinct excitation energies: (a) at the exciton resonance  $h\nu_\tau = E_E$ , and (b) free carrier excitation  $h\nu_\tau > E_G$ . Profiles correspond to horizontal cuts along 2D spectra in Fig. 2 showing the transient dynamics at additional pump-probe delay steps  $\Delta t$ . Free-carrier excitation and Coulomb renormalization of the excitonic transition, causing the derivative-shape spectral profile of differential transmission [Fig. 3(b)], is instantaneous and remains steady in the range of investigated delay times owing to the slow ( $> 100$  ps) carrier relaxation. In contrast, excitation resonant to the excitonic transition at 2 eV [Fig. 3(a)] emphasizes the ultrafast exciton dynamics captured by the fast relaxation of the predominantly positive peak associated to the bleaching of the transition. In addition to the shifting and bleaching illustrated in Fig. 1(c), our data may contain a transient increase of the exciton linewidth at sub-50-fs delay identified by a differential transmission proportional to the second derivative of the excitonic absorption, as highlighted with black arrows for  $\Delta t = 20$  fs in Fig. 3(a). The limitation of this effect to resonant excitation [not seen at higher excitation energy in Fig. 3(b)] directly relates it to the exciton population of the system, also known as excitation induced dephasing [12,39], which can dominate bleaching at short delay [40]. At time delays  $\Delta t \geq 500$  fs, the bleaching effect fully disappears and spectral profiles resulting from free-carrier and exciton

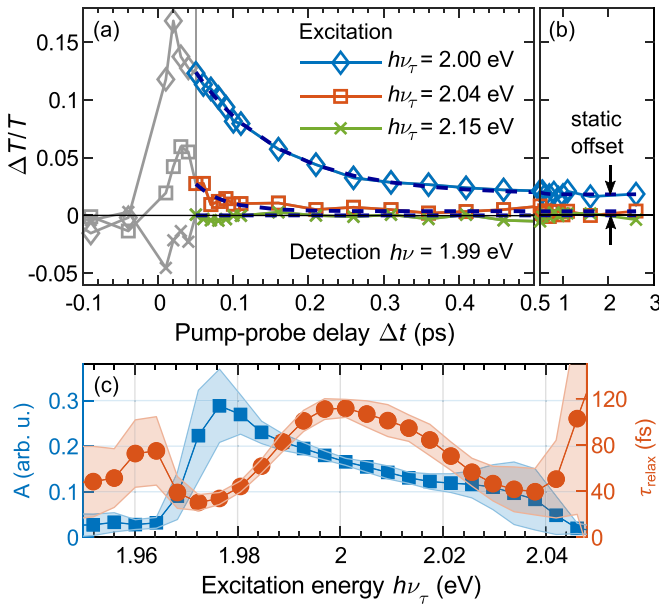


FIG. 4. (a),(b) Ultrafast relaxation of differential transmission change  $\Delta T/T$  extracted at the position of colored circles in Fig. 2. Dashed lines (dark blue) show an exponential fit as described in the text. Gray data points ( $\Delta t < 50$  fs) are not included for the fit. (c) Fit amplitude  $A$  (squares) and relaxation time  $\tau_{\text{relax}}$  (circles) as a function of excitation energy. Shaded areas denote the fit uncertainty.

excitations appear strikingly similar, with minor differences discussed in the following.

The ability to distinguish precisely the ultrafast optical response related to different excitation energies within the broadband spectrum is a key ingredient to fully explore and understand the carrier dynamics of functional materials. The combination of energy resolution enabled by 2D electronic spectroscopy and exceptional sensitivity in the experiment allow us to focus our attention to extremely narrow spectral features of the 2D map. Figures 4(a) and 4(b) show the temporal evolution of differential signals extracted at different spectral positions, highlighted by colored circles in Fig. 2(c), using a 2D Gaussian filter with 1 THz (4 meV) FWHM spectral bandwidth. The spectral interval of detection energy for this analysis is centered at 1.99 eV and chosen such that the optical response from free carriers at  $h\nu_{\tau} > 2.15$  eV levels to zero. By choosing the excitation energy resonant to the exciton transition, a strong and clear signal arises. An exponential fit  $\Delta T/T(\Delta t) = A \exp(-\Delta t/\tau_{\text{relax}}) + C$  captures the ultrafast relaxation, providing amplitude  $A$ , relaxation time  $\tau_{\text{relax}}$ , and a static offset  $C$  as a function of excitation energy. Figure 4(c) presents the dependence of fit parameters on excitation energy in the vicinity of the exciton resonance, with shaded areas denoting the fit uncertainty. The relaxation time reaches a maximum  $\tau_{\text{relax}} = 112(\pm 8)$  fs at  $h\nu_{\tau} = 2$  eV, revealing the most efficient excitation of excitons, which we identify with the thermal dissociation of excitons to free carriers  $\tau_E$ . A slightly increased signal amplitude at energies just below this resonance relates to a reduced density of states in the band structure and hence a stronger differential signature of the bleaching process.

The offset  $C$  of the transient signal at resonant excitation energy highlighted in Fig. 4(b) is inherent to our measurements and remains static in the range of investigated delays. It relates to a weak static bleach near the band edge caused by the increased lattice temperature that becomes insignificant at reduced excitation pulse fluence  $< 1 \text{ mJ/cm}^2$ . At very short delays ( $\Delta t < 50$  fs), when the exciton population is high, the encircled area of the 2D spectrum in Fig. 2(a) highlights photoinduced absorption (PIA) at photon energies of interband free-carrier excitations. This transient increase of absorption is related to the strong depopulation of electronic states near the valence band edge when pumping the system at high fluence, which recovers with refilling through intraband carrier scattering within 100 fs of the excitation.

Independent measurements with different sample thickness reveal identical relaxation dynamics. At reduced excitation pulse fluence ( $0.6 \text{ mJ/cm}^2$ ), we find an exciton relaxation time of  $113(\pm 9)$  fs (not shown). Considering a reduction of excitation fluence by a factor of 3, this confirms that the observed effect is nonthermal and widely independent of carrier population in the material. By setting the lower fit limit to 50 fs (vertical line), thereby not including coherent effects near the overlap, the extracted exciton relaxation time is identical for all measurements and at all investigated fluences underlining a negligible dependence on carrier population for this relaxation process. Indirect excitons at the  $M$  point of the Brillouin zone, which have 10 meV lower excitation energy [41], remain inaccessible in the experiment due to insufficient momentum of photons.

In conclusion, we have shown how 2D electronic spectroscopy is capable to disentangle ultrafast dynamics in a semiconductor with 10 fs temporal and down to 1 THz (4 meV) spectral resolution in the visible frequency range. The higher dimensionality of the data obtained with our three-pulse experiment allows us to precisely determine the optical response as function of excitation frequency without sacrificing temporal resolution. In an optically thin but bulk sample of GaSe, we were able to extract the precise lifetime of the excitonic ground state at room temperature, which is  $112(\pm 8)$  fs with resonant excitation at 2 eV. The presence of bound excitons manifests itself in a transient reduction of absorption at the exciton resonance. This feature is not noticeable in standard pump-probe measurements due to the broadband nature of ultrashort pulses that causes a dominant response from free carriers. Our sophisticated phasing and calibration procedures allow us to reconstruct the differential transmission in 2D spectra independent of the spectral pulse profiles, and hence provide valuable information beyond the pure temporal dynamics. We envision to target GaSe thin films and other 2D materials in future experiments [24].

The experiments in GaSe discussed throughout this work strikingly demonstrate the power of this technique and its applicability to bulk solid-state materials in order to disentangle the distinct exciton and free-carrier dynamics in a bulk semiconductor. The quantitative mapping of interesting features seen in 2D spectra especially at short delay motivates ongoing theoretical investigations. Our findings pave the way for future investigation of materials exploring energetic and quasiparticle correlations.



We gratefully acknowledge scientific discussion with Dr. A. Leitenstorfer. This work was supported by the Emmy Noether Program of the DFG (Grant No. BR 5030/1-1) and the FEDER Program (Grant No. 2017-03-022-19 “Lux-Ultra-Fast”).

- [1] K. S. Novoselov, A. Mishchenko, A. Carvalho, and A. H. Castro Neto, 2D materials and van der waals heterostructures, *Science* (80-.). **353**, aac9439 (2016).
- [2] J. Cheng, C. Wang, X. Zou, and L. Liao, Recent advances in optoelectronic devices based on 2D materials and their heterostructures, *Adv. Opt. Mater.* **7**, 1800441 (2019).
- [3] E. Cassette, J. C. Dean, and G. D. Scholes, Two-Dimensional visible spectroscopy for studying colloidal semiconductor nanocrystals, *Small* **12**, 2234 (2016).
- [4] A. Grupp, A. Budweg, M. P. Fischer, J. Allerbeck, G. Soavi, A. Leitenstorfer, and D. Brida, Broadly tunable ultrafast pump-probe system operating at multi-KHz repetition rate, *J. Opt.* **20**, 014005 (2018).
- [5] S. T. Cundiff and S. Mukamel, Multidimensional coherent spectroscopy, *Physics Today* **66**(7), 44 (2013).
- [6] P. Hamm and M. T. Zanni, *Concepts and Methods of 2D Infrared Spectroscopy* (Cambridge University Press, Cambridge, UK, 2011).
- [7] R. M. Hochstrasser, Two-Dimensional spectroscopy at infrared and optical frequencies, *Proc. Natl. Acad. Sci. USA* **104**, 14190 (2007).
- [8] D. B. Turner, Y. Hassan, and G. D. Scholes, Exciton superposition states in CdSe nanocrystals measured using broadband Two-Dimensional electronic spectroscopy, *Nano Lett.* **12**, 880 (2012).
- [9] L. Guo, M. Wu, T. Cao, D. M. Monahan, Y. H. Lee, S. G. Louie, and G. R. Fleming, Exchange-driven intravalley mixing of excitons in monolayer transition metal dichalcogenides, *Nat. Phys.* **15**, 228 (2019).
- [10] S. T. Cundiff, Coherent spectroscopy of semiconductors, *Opt. Express* **16**, 4639 (2008).
- [11] S. T. Cundiff, Optical two-dimensional fourier transform spectroscopy of semiconductor nanostructures [invited], *J. Opt. Soc. Am. B* **29**, A69 (2012).
- [12] X. Li, T. Zhang, C. N. Borca, and S. T. Cundiff, Many-Body Interactions In Semiconductors Probed By Optical Two-Dimensional Fourier Transform Spectroscopy, *Phys. Rev. Lett.* **96**, 057406 (2006).
- [13] E. Cassette, R. D. Pensack, B. Mahler, and G. D. Scholes, Room-temperature exciton coherence and dephasing in two-dimensional nanostructures, *Nat. Commun.* **6**, 6086 (2015).
- [14] J. M. Richter, F. Branchi, F. Valduga De Almeida Camargo, B. Zhao, R. H. Friend, G. Cerullo, and F. Deschler, Ultrafast carrier thermalization in lead iodide perovskite probed with two-dimensional electronic spectroscopy, *Nat. Commun.* **8**, 376 (2017).
- [15] A. Jha, H. G. Duan, V. Tiwari, P. K. Nayak, H. J. Snaith, M. Thorwart, and R. J. Dwayne Miller, Direct observation of ultrafast exciton dissociation in lead iodide perovskite by 2d electronic spectroscopy, *ACS Photonics* **5**, 852 (2018).
- [16] A. De Sio, F. Troiani, M. Maiuri, J. Réhault, E. Sommer, J. Lim, S. F. Huelga, M. B. Plenio, C. A. Rozzi, G. Cerullo, E. Molinari, and C. Lienau, Tracking the coherent generation of polaron pairs in conjugated polymers, *Nat. Commun.* **7**, 13742 (2016).
- [17] A. DeSio and C. Lienau, Vibronic coupling in organic semiconductors for photovoltaics, *Phys. Chem. Chem. Phys.* **19**, 18813 (2017).
- [18] F. Milota, J. Sperling, A. Nemeth, T. Mančal, and H. F. Kauffmann, Two-dimensional electronic spectroscopy of molecular excitons, *Acc. Chem. Res.* **42**, 1364 (2009).
- [19] F. Junginger, A. Sell, O. Schubert, B. Mayer, D. Brida, M. Marangoni, G. Cerullo, A. Leitenstorfer, and R. Huber, Single-cycle multiterahertz transients with peak fields above 10 MV/Cm, *Opt. Lett.* **35**, 2645 (2010).
- [20] O. Schubert, M. Hohenleutner, F. Langer, B. Urbanek, C. Lange, U. Huttner, D. Golde, T. Meier, M. Kira, S. W. Koch, and R. Huber, Sub-cycle control of terahertz high-harmonic generation by dynamical bloch oscillations, *Nat. Photonics* **8**, 119 (2014).
- [21] K. R. Allakhverdiev, M. Ö. Yetis, S. Özbek, T. K. Baykara, and E. Y. Salaev, Effective nonlinear gas crystal. optical properties and applications, *Laser Phys.* **19**, 1092 (2009).
- [22] P. Hu, Z. Wen, L. Wang, P. Tan, and K. Xiao, Synthesis of few-layer gase nanosheets for high performance photodetectors, *ACS Nano* **6**, 5988 (2012).
- [23] Y. Cao, K. Cai, P. Hu, L. Zhao, T. Yan, W. Luo, X. Zhang, X. Wu, K. Wang, and H. Zheng, Strong enhancement of photoreponsivity with shrinking the electrodes spacing in few layer GaSe photodetectors, *Sci. Rep.* **5**, 08130 (2015).
- [24] A. Budweg, D. Yadav, A. Grupp, A. Leitenstorfer, M. Trushin, F. Pauly, and D. Brida, Control of excitonic absorption by thickness variation in Few-Layer GaSe, *Phys. Rev. B* **100**, 045404 (2019).
- [25] R. Longuinhos and J. Ribeiro-Soares, Ultra-weak interlayer coupling in two-dimensional gallium selenide, *Phys. Chem. Chem. Phys.* **18**, 25401 (2016).
- [26] D. J. Late, B. Liu, J. Luo, A. Yan, H. S. S. R. Matte, M. Grayson, C. N. R. Rao, and V. P. Dravid, GaS and GaSe ultrathin layer transistors, *Adv. Mater.* **24**, 3549 (2012).
- [27] P. Dey, J. Paul, G. Moody, C. E. Stevens, N. Glikin, Z. D. Kovalyuk, Z. R. Kudrynskiy, A. H. Romero, A. Cantarero, D. J. Hilton, and D. Karaiskaj, Biexciton formation and exciton coherent coupling in layered GaSe, *J. Chem. Phys.* **142**, 212422 (2015).
- [28] D. Brida, C. Manzoni, and G. Cerullo, Phase-locked pulses for two-dimensional spectroscopy by a birefringent delay line, *Opt. Lett.* **37**, 3027 (2012).
- [29] M. Schlüter, J. Camassel, S. Kohn, J. P. Voitchovsky, Y. R. Shen, and M. L. Cohen, Optical properties of GaSe and Ga-Sx-Se(1-x) mixed crystals, *Phys. Rev. B* **13**, 3534 (1976).
- [30] R. LeToullec, N. Piccioli, and J. C. Chervin, Optical properties of the band-edge exciton in GaSe crystals at 10 K, *Phys. Rev. B* **22**, 6162 (1980).
- [31] J. V. McCanny and R. B. Murray, The band structures of Gallium and Indium selenide, *J. Phys. C: Solid State Phys.* **10**, 1211 (1977).
- [32] A. M. Bakiev, Y. V. Vandyshev, G. S. Volkov, V. S. Dneprovskil, Z. D. Kovalyuk, A. R. Lesiv, S. V. Savinov, and A. I. Furtichev,

- Screening of excitons in semiconductor GaSe, *Fiz. Tverd. Tela* **28**, 1035 (1986) [*Sov. Phys. Solid State* **28**, 579 (1986)].
- [33] D. C. Reynolds, D. C. Look, and B. Jogai, Combined effects of screening and band gap renormalization on the energy of optical transitions in ZnO and GaN, *J. Appl. Phys.* **88**, 5760 (2000).
- [34] B. Mayer, C. Schmidt, J. Bühler, D. V. Seletskiy, D. Brida, A. Pashkin, and A. Leitenstorfer, Sub-cycle slicing of phase-locked and intense mid-infrared transients, *New J. Phys.* **16**, 063033 (2014).
- [35] P. C. Becker, H. L. Fragnito, C. H. B. Cruz, R. L. Fork, J. E. Cunningham, J. E. Henry, and C. V. Shank, Femtosecond Photon Echoes From Band-To-Band Transitions in GaAs, *Phys. Rev. Lett.* **61**, 1647 (1988).
- [36] S. L. Sewall, R. R. Cooney, K. E. H. Anderson, E. A. Dias, and P. Kambhampati, State-to-state exciton dynamics in semiconductor quantum dots, *Phys. Rev. B* **74**, 235328 (2006).
- [37] Y. Yan, G. Chen, and P. G. Van Patten, Ultrafast exciton dynamics in CdTe nanocrystals and Core/Shell CdTe/CdS nanocrystals, *J. Phys. Chem. C* **115**, 22717 (2011).
- [38] J. Madéo, M. K. L. Man, C. Sahoo, M. Campbell, V. Pareek, E. L. Wong, A. Al-Mahboob, N. S. Chan, A. Karmakar, B. M. K. Mariserla, X. Li, T. F. Heinz, T. Cao, and K. M. Dani, Directly visualizing the momentum-forbidden dark excitons and their dynamics in atomically thin semiconductors, *Science* (80-). **370**, 1199 (2020).
- [39] H. Wang, K. Ferrio, D. G. Steel, Y. Z. Hu, R. Binder, and S. W. Koch, Transient Nonlinear Optical Response From Excitation Induced Dephasing in GaAs, *Phys. Rev. Lett.* **71**, 1261 (1993).
- [40] D. B. Turner, P. Wen, D. H. Arias, K. A. Nelson, H. Li, G. Moody, M. E. Siemens, S. T. Cundiff, X. Li, T. Zhang, C. N. Borca, and S. T. Cundiff, Persistent Exciton-Type Many-Body Interactions in GaAs Quantum Wells Measured Using Two-Dimensional Optical Spectroscopy, *Phys. Rev. B* **85**, 201303(R) (2012).
- [41] V. Capozzi, L. Pavesi, and J. L. Staehli, Exciton-carrier scattering in gallium selenide, *Phys. Rev. B* **47**, 6340 (1993).